Tree Physiology 26, 1445–1456

Modeling photosynthesis in olive leaves under drought conditions

A. DÍAZ-ESPEJO,[1,2] A. S. WALCROFT,[3] J. E. FERNÁNDEZ,[1] B. HAFIDI,[1] M. J. PALOMO[1] and I. F. GIRÓN[1]

[1] *Instituto de Recursos Naturales y Agrobiología, CSIC, Apartado 1052, 41080 Sevilla, Spain*

[2] *Corresponding author (adiaz@irnase.csic.es)*

[3] *Landcare Research, Private Bag 11052, Riddet Road, Massey University, Palmerston North, New Zealand*

Received September 16, 2005; accepted February 18, 2006; published online August 1, 2006

Summary We quantified parameters for a model of leaf-level photosynthesis for olive, and tested the model against an independent dataset. Specific temperature-dependence parameters of the model for olive leaves were measured, as well as the relationship of the model parameters with area-based leaf nitrogen (N) content. The effect of soil water deficit on leaf photosynthesis was examined by applying two irrigation treatments to 29-year-old trees growing in a plantation: drip irrigation sufficient to meet the crop water requirements (I) and dry-farming (D). In both treatments, leaves had a higher photosynthetic capacity in April than in August. In August, photosynthetic capacity was lower in D trees than in I trees. Leaf photosynthetic capacity was linearly and positively related to leaf N content on an area basis (N_a) and to leaf mass per unit area (LMA), and the regression slope varied with irrigation treatment. The seasonal reduction in N_a was used in the model to predict photosynthesis under drought conditions. Olive leaves showed a clear limitation of photosynthesis by triose phosphate utilization (TPU) even at 40 °C, and the data suggest that olive invests fewer resources in TPU than other species. The seasonal decrease in photosynthetic capacity moderated the stomatal limitation to carbon dioxide (CO_2) fixation as soil water deficit increased. Further, it enabled leaves to operate close to the transition point between photosynthetic limitation due to RuBP carboxylation capacity and that due to RuBP regeneration capacity, and resulted in a near constant value of internal CO_2 concentration from April to August. Under well watered conditions, N-use efficiency of the olive leaves was enhanced at the expense of reduced water-use efficiency.

Keywords: leaf nitrogen, nitrogen-use efficiency, non-stomatal limitation, Olea europaea, triose phosphate utilization, water-use efficiency.

Introduction

Olive (*Olea europaea* L.) is one of the most important cultivated fruit tree species in the Mediterranean region. World demand for olive products, both oil and fruit, is increasing because of their nutritional properties. The ability of olive trees to grow in arid and semiarid regions makes this species important for minimizing erosion and desertification, and for improving the carbon balance of these areas.

Most studies on the physiology of olive trees have focused on the responses of this species to stress under both controlled (Tombesi et al. 1984, Bongi et al. 1987, Angelopoulos et al. 1996, Dichio et al. 1997) and field conditions (Larsen et al. 1989, Goldhamer et al. 1994, Michelakis et al. 1996, Moreno et al. 1996, Fernández et al. 1997, Fernández and Moreno 1999). Although much is known about the mechanisms involved in the responses of olive to different stresses, it is difficult to evaluate the individual contribution of each one to the whole-plant response, because of the large number of environmental factors operating simultaneously under field conditions.

Crop modeling has become a major research tool in horticulture (Gary et al. 1998). Simulation models are being used to understand the integration of physiological processes and mechanisms of response to stress, and to evaluate the consequences of this integration at different temporal and spatial scales. Models help to interpret experimental results gained under different environmental conditions and to develop and test new production technologies (Pokovai and Kovacs 2003). Crop modeling is particularly relevant to olive groves, because olives have traditionally been grown under dry-farming conditions but are now being grown under irrigated conditions (Fergusson 2000).

As a result of the improvements in production brought about by irrigation (Lavee et al. 1990, Goldhamer et al. 1994), there is a need to better understand the physiology of olive responses to irrigation. Fergusson (2000) highlighted the need to develop mechanistic models representing physiological and physical processes in olive trees. Such models can help in understanding and improving irrigation practices, pruning and the design of commercial orchards. Moreno et al. (1996) obtained good agreement between modeled transpiration rates of olive trees based on the Penman–Monteith equation, considering sunlit and shaded leaf areas, and transpiration rates measured by the sap flow technique. Villalobos et al. (2000) used the eddy covariance method to estimate sensible and latent heat flux above and below the trees. At the tree level, two models have been proposed for olive that describe radiation interception

(Mariscal et al. 2000*a*) and radiation use-efficiency and dry matter partitioning (Mariscal et al. 2000*b*). Díaz-Espejo et al. (2002) modeled the radiation regime in an olive crown, and estimated transpiration and photosynthesis of a mature olive tree. At the leaf level, Moriana et al. (2002) calibrated three stomatal conductance models for olive and concluded that the model described by Leuning (1995), in which photosynthesis and stomatal conductance are explicitly linked, performed best. However, a mechanistic model of photosynthesis has not yet been fully described.

The aim of this work was to develop a leaf-level model of photosynthesis that would allow carbon dioxide (CO_2) assimilation rate (A) of a mature olive tree under field conditions to be predicted as a function of the driving environmental variables. Particular attention was paid to measuring the effect of drought on A. Gas-exchange measurements were used to determine parameter values for the Farquhar et al. (1980) photosynthesis model. This model was linked to a model of stomatal conductance (Jarvis 1976), in which an effect of soil water deficit has been included. Parameters were initially determined on 2-year-old seedlings. To ensure the generality of the model parameters, additional measurements were performed on leaves of 29-year-old trees under field conditions. The relationship between area-based nitrogen (N) content and photosynthetic capacity of the leaves, as well as their seasonal development, were evaluated in field-grown trees under both water-stress and well-watered conditions.

Materials and methods

Model description

To model A as a function of environmental conditions, we used the approach of Farquhar et al. (1980), including the potential phosphate limitation presented by Harley and Tenhunen (1991):

$$A = \min\{A_c, A_q, A_p\} - R_d \quad (1)$$

where A_c (μmol m^{-2} s^{-1}) is the rate of photosynthesis limited by the RuBP (ribulose bisphosphate) carboxylation activity of the enzyme Rubisco (ribulose-1,5-bisphosphate carboxylase oxygenase), A_q (μmol m^{-2} s^{-1}) is the rate of photosynthesis limited by RuBP regeneration via electron transport, A_p (μmol m^{-2} s^{-1}) is the rate of photosynthesis limited solely by inorganic phosphate, and R_d is the rate of CO_2 evolution in the light resulting from processes other than photorespiration.

When Rubisco activity is limiting, assimilation rate is given by:

$$A_c = V_{cmax}\frac{C_i - \Gamma^*}{C_i + K_c[1 + (o_i / K_o)]} \quad (2)$$

where V_{cmax} is maximum catalytic activity of Rubisco in the presence of saturating amounts of RuBP and CO_2, C_i is the intercellular CO_2 mole fraction, Γ^* is the CO_2 compensation point in the absence of R_d, o_i is the intercellular O_2 mole fraction, and K_c and K_o are Michaelis constants for CO_2 and O_2, respectively.

When photosynthetic electron transport limits RuBP regeneration, assimilation rate is given by:

$$A_q = \frac{J(C_i - \Gamma^*)}{4(C_i + 2\Gamma^*)} \quad (3)$$

where J is rate of electron transport for a given absorbed photon irradiance (photosynthetic photon flux; PPF). A nonrectangular hyperbolic function (Farquhar and Wong 1984) was used to calculate J as a function of PPF:

$$\theta J^2 - (\alpha \mathrm{PPF} + J_{max})J + \alpha \mathrm{PPF} J_{max} = 0 \quad (4)$$

where θ describes the degree of curvature of the function, α is the quantum efficiency of electron transport and J_{max} is the maximum rate of electron transport at saturating irradiance.

Finally, A_p defines assimilation limited by regeneration of RuBP under conditions of low inorganic phosphate (P_i) availability (Harley and Tenhunen 1991):

$$A_p = \frac{3\mathrm{TPU}}{\left(1 - \frac{\Gamma^*}{C_i}\right)} \quad (5)$$

where TPU is the rate of P_i release associated with triose phosphate utilization.

The temperature dependencies of V_{cmax}, J_{max}, TPU, Γ^*, K_c, K_o and R_d are described by an exponential function (Bernacchi et al. 2001):

$$\text{Parameter} = \exp[(c - \Delta H_a / R(T_l + 273)] \quad (6)$$

where R is the molar gas constant and T_l is leaf temperature (°C). The terms c and ΔH_a represent a scaling constant and an activation energy, respectively.

Table 1. Values and units of the parameters used in the photosynthesis model for olive.

Parameter	Value	Units
θ	0.9[1]	–
α	0.2[1]	mol e mol^{-1} quanta
cK_c	38.05[2]	–
cK_{o0}	20.30[2]	–
$\Delta H_a K_c$	79.43[2]	KJ mol^{-1}
$\Delta H_a K_o$	36.38[2]	KJ mol^{-1}
$c\Gamma^*$	19.02[2]	–
$\Delta H_a \Gamma^*$	37.83[2]	KJ mol^{-1}

[1] Measured in this study.
[2] From Bernacchi et al. (2001).

Values of the parameters used in the C_3 photosynthesis model are given in Table 1. The photosynthesis model was coupled to a model of stomatal conductance, with parameters determined specifically for olive (Diaz-Espejo et al. 2002). Briefly, the stomatal response to environmental variables (i.e., stomatal conductance to water vapor; g_s) was modeled following the approach of Jarvis (1976):

$$g_s = g_{sref} f(PPF) f(T_l) f(VPD) f(SWC) \quad (7)$$

where g_{sref} (mol m^{-2} s^{-1}) is the reference stomatal conductance observed under standard conditions (PPF = 1600 μmol m^{-2} s^{-1}; T_l = 25 °C; VPD = 1 kPa; and SWC = 0.19 m^3 m^{-3}), T_l (°C) is leaf temperature, VPD (kPa) is air water vapor pressure deficit, and SWC is volumetric soil water content (m^3 m^{-3}). Details of functions used in the stomatal conductance model for olive are given in the Appendix and in Diaz-Espejo et al. (2002).

The photosynthesis and stomatal conductance models are coupled through C_i:

$$C_i = C_a - A/g_{sc} \quad (8)$$

where C_a is mole fraction of CO_2 in ambient air and g_{sc} is stomatal conductance to CO_2 ($g_{sc} = g_{sw}/1.6$). Equations 1–3 were solved analytically following Wang and Jarvis (1993).

Model parameterization

Twenty-five 2-year-old olive trees were planted in 4.5-l pots in the spring of 1999 and placed in a greenhouse at the Instituto de Recursos Naturales y Agrobiología (Seville, Spain) from March to August. The pots were filled with soil from the experimental farm nearby, with the aim of matching conditions in the field. All pots were watered to saturation every second day and supplied with Hoagland's nutrient solution once per week. Temperature in the greenhouse ranged between 14 and 32 °C from March to May and between 22 and 42 °C from June to August. Maximum incident PPF (μmol m^{-2} s^{-1}) recorded was 1900 μmol m^{-2} s^{-1}. Soil water content was measured in four pots by time-domain reflectometry (TDR) with a Tektronix cable tester (Model 1502C, Beaverton, OR). Three TDR probes per pot were installed permanently. Measurements indicated that the irrigation frequency maintained SWC around 0.21 corresponding to a soil matric potential (Ψ_m) of about –0.01 MPa.

Measurements of the response of A to temperature were made with two portable photosynthesis systems (LI-6400, Li-Cor, Lincoln NE) that allow environmental conditions inside the cuvette to be precisely controlled. Three plants were placed in a phytotron growth cabinet on the evening before the gas exchange measurements. Air temperature in the growth chamber was set at 15, 20, 25, 30, 35 and 40 °C, and PPF and humidity were maintained at 1000 μmol m^{-2} s^{-1} and 70%, respectively, across all temperatures. In the cuvette, VPD varied between 0.5 and 1.7 kPa in response to the changes in cuvette air temperature. Five A/PPF response curves were measured at ambient CO_2 concentration to determine quantum yield and the saturating irradiance. Six A/C_i response curves were made at the saturating irradiance (PPF = 1600 μmol m^{-2} s^{-1}) for each temperature. Each response curve was measured on a leaf from a different plant, and each plant spent no longer than 24 h in the growth cabinet. Leaf respiration was measured with the chamber lights off, as the rate of CO_2 evolution. Each A/C_i curve was performed by varying the leaf chamber CO_2 concentration between 50 and 1400 μmol mol^{-1} in at least 11 steps. Values of A and C_i were recorded from ambient CO_2 to 50 μmol mol^{-1}, and then returned to ambient CO_2 concentration to check that the original A could be restored. If this was achieved, then CO_2 concentration was increased stepwise to 1400 μmol mol^{-1} until the curve was completed. At saturating PPF and low C_i, carboxylation is assumed to be limited solely by Rubisco activity. The parameters V_{cmax} and R_d were determined by fitting Equation 2 to the response curve where C_i < 250 μmol mol^{-1}. As C_i increases, A becomes limited by the rate of electron transport or by the turnover rate of inorganic phosphate. The parameters J_{max} and TPU were determined by fitting Equation 1 to the whole response curve, based on the previously determined values for V_{cmax} and R_d. Analysis of TPU limitation was only undertaken on A/C_i responses showing a decline in A at high C_i. The measured leaves were collected for measurement of leaf dry mass, leaf area and total organic N concentration. Leaf area was measured with a Delta-T Image Analysis System (Delta-T Devices, Cambridge, U.K.). Leaf N content was determined by a micro-Kjeldahl assay and expressed on a leaf area basis.

Field measurements and model validation

Field experiments were carried out at La Hampa experimental farm (37°17′ N, 6°3′ W; altitude 30 m), near Seville, Spain. The 1-ha experimental orchard contained 29-year-old olive trees (*Olea europaea* L., 'Manzanilla') at a spacing of 7 × 7 m. The soil is a sandy loam (Xerochrept) of a depth varying between 0.9–2 m. Below that, a hard carbonaceous sandstone pan impedes the penetration of both roots and water. The texture of the root zone is quite homogeneous with average values of 73.5% coarse sand, 4.7% fine sand, 7% silt and 14.8% clay. The values of SWC at field capacity (–0.01 MPa) and wilting point (–1.5 MPa) were 0.21 and 0.10, respectively.

Two watering regimes were imposed: (1) Treatment D (Dry-farming) in which rainfall was the only source of water; and (2) Treatment I (Irrigated), where daily irrigation replaced the crop water demand (ET_c, mm) as calculated by the equation $ET_c = K_r K_c ET_o$, where ET_o is the potential evapotranspiration (mm) calculated from weather station measurements made at the farm (see below). The values of K_r and K_c were previously adjusted for the orchard conditions, as described by Palomo et al. (2002). The irrigation seasons extended from mid March to the beginning of October. Water was supplied to the I trees by a drip irrigation system consisting of a single pipe per tree row, with five 3 l h^{-1} drippers per tree, 1 m apart. The trees in treatment I had been irrigated regularly since they were planted.

Meteorological variables were measured with an automatic weather station located 50 m away from the experimental

trees. Thirty-minute means of net radiation, global radiation, photosynthetically active radiation, wind speed, rainfall, air temperature and relative humidity were recorded.

Soil water content was estimated for three trees per water treatment. Measurements were made with a neutron probe (Troxler 3300, Research Triangle Park, NC) with access tubes installed at 0.5, 1.5, 2.5 and 3.5 m from the trunk of each tree. Measurements of SWC were made every 0.1 m from 0.2–2.0 m. In the top layer, SWC was estimated by gravimetric measurements and then converted into volumetric data using the soil bulk density measured in the field. Soil water content was measured every 10–15 days.

Leaf water status was evaluated as leaf water potential (Ψ_w, MPa) measured with a pressure chamber (Soilmoisture Equipment Corp, Santa Barbara, CA), and as the relative water content (RWC) of the leaves. Net photosynthesis and g_s were measured one day per month from March to August 1998 with a Li-Cor LI-6400. Measurements were made every 2 h from dawn to sunset. Six leaves were sampled from five trees per treatment for Ψ_w, and ten leaves for RWC, g_s and A. All physiological measurements were performed on fully expanded current-year leaves located in sun-exposed parts of the canopy. The survey measurements provided an independent data set to validate the photosynthesis and stomatal conductance models. In March, the measurements were made on previous-year leaves, because there were no fully expanded current-year leaves at that time of the year.

Six A/C_i curves per treatment were made to determine the photosynthetic capacity of leaves of mature olive trees under field conditions. A set of curves was made in April and another set in August when soil water deficit in treatment D had increased. A scaffold tower was erected to gain access to leaves at different orientations and locations. Response curves were made at 25 °C, and leaves were collected following measurements for analyses of leaf area and N content.

The photosynthesis model was validated against the independent dataset of A and g_s measurements made in the orchard, in trees in both watering treatments. The model was run for the same days on which the measurements were made. Calculations were performed on a half-hourly time step using measured PPF, air temperature and humidity, and assuming the leaf was fully exposed to sunlight. Values of SWC input into the model were the average of the water profiles measured in the soil volume where roots were active. Thus, the top soil layer of D treatment was not considered, because changes in SWC with time were negligible. The daily pattern of C_a was obtained from the survey gas exchange measurements.

An index of stomatal limitation to photosynthesis (l_g, %) was calculated (Jones 1992) as:

$$l_g = r_g/(r_g + r*) \times 100 \quad (9)$$

where r_g is the gas-phase CO_2 transfer resistance ($1/g_{sc}$), which defines the CO_2 supply function, and $r*$ is the inverse slope of the A/C_i response, $(dA/dC_i)^{-1}$, at the operating point, which is where the supply function intercepts the A/C_i response function.

Results

Temperature effect

An increase in T_l affected both the initial slopes of the A/C_i curves (carboxylation efficiency) and the maximum photosynthetic rate (Figure 1). At low temperatures, the transition between RuBP carboxylation-limited and RuBP regeneration-limited photosynthesis was achieved at lower CO_2 concentrations than at high temperatures (237 μmol mol^{-1} at 15 °C; 353 μmol mol^{-1} at 35 °C). Maximum values of A were recorded at 35 °C. The CO_2 compensation point (Γ) also increased with T_l from 35.2 μmol mol^{-1} at 15 °C to 71.4 μmol mol^{-1} at 35 °C.

Model parameters V_{cmax}, J_{max}, TPU and R_d were all strongly influenced by T_l (Figure 2). The exponential equation proposed by Bernacchi et al. (2001) explained a high proportion of the variance observed (R^2 up to 0.95; $P < 0.001$). The need for a peaked function using an extra deactivation parameter, H_d, was analyzed with the dataset for V_{cmax}, J_{max} and calculated based on Bernacchi's approach (data not shown). The addition of H_d did not significantly increase the proportion of variance explained by the model ($P = 1.0$ for V_{cmax} and J_{max}). For TPU, the peak function increased the proportion of variance explained only slightly ($P < 0.001$; R^2 increased from 0.88 to 0.90). Specific values of the temperature-dependence parameters for olive are shown in Table 2.

Temperature had a greater effect on V_{cmax} than on J_{max} and TPU. Values of V_{cmax} increased 10-fold between 15 and 40 °C, whereas J_{max} and TPU increased by 3-fold, resulting in declines in the ratios of J_{max}:V_{cmax} (Figure 3) and TPU:V_{cmax}. An exponential function explained the greatest proportion of the observed variance in the relationships between temperature and the ratios J_{max}:V_{cmax} and TPU:V_{cmax} ($R^2 = 0.95$). However, a linear function better described the relationship between J_{max}:TPU and temperature ($r^2 = 0.75$; $P < 0.001$).

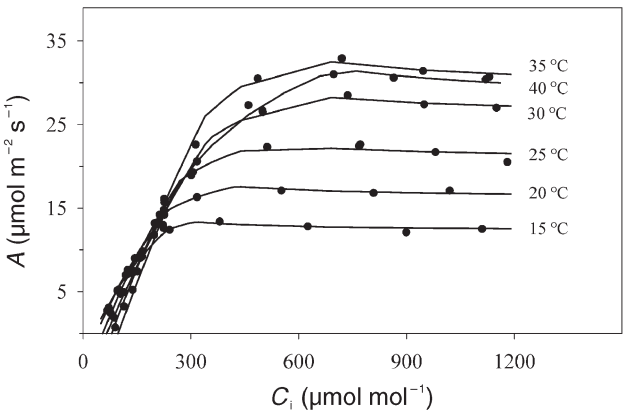

Figure 1. The A/C_i response curves for olive at different temperatures. Six curves were made for each temperature but only a representative curve is shown for simplicity. The graph shows the limitation imposed on photosynthetic rate (A) at 500 μmol mol^{-1} internal CO_2 (C_i) by the regeneration of ribulose biphosphate due to phosphate availability. Each value represents an individual measurement. Solid lines represent model fits.

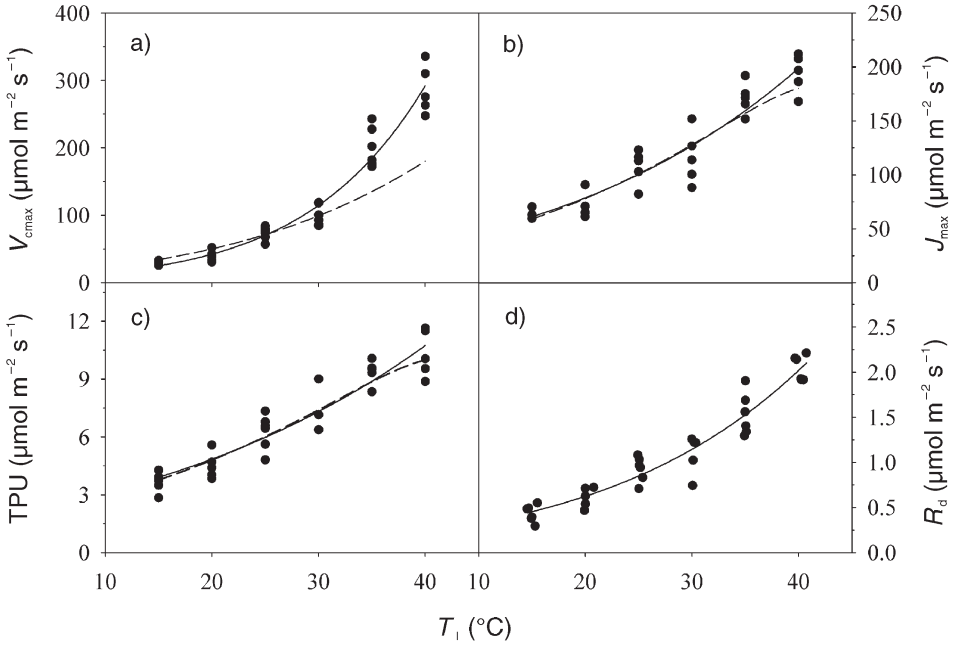

Figure 2. Response to olive leaf temperature (T_l) of the photosynthesis model parameters (a) maximum catalytic activity of Rubisco in the presence of saturating amounts of RuBP and CO_2 (V_{cmax}); (b) maximum rate of electron transport at saturating irradiance (J_{max}); (c) rate of P_i release associated with triose phosphate utilization (TPU); and (d) rate of CO_2 evolution in the light (R_d). Each value represent an individual measurement made on a different plant. Solid line represents model fits with in vivo parameters from Bernacchi et al. (2001). Broken line represents model fits with in vitro parameters from Badger and Collatz (1977).

Values of R_d increased exponentially with T_l (Figure 2). The values of R_d estimated from CO_2 efflux in darkness were compared to estimates of R_d derived by fitting the model equation for A_c. The values of R_d at each temperature were more variable with the second technique; however, the values of R_d at 25 °C and H_aR_d estimated with both techniques were similar.

Leaf nitrogen effect

The parameters V_{cmax}, J_{max}, TPU and R_d were all linearly related to leaf N expressed on an area basis (N_a) for both the field-grown trees and the potted plants (Figure 4). Values of N_a declined over time from 5.33 g m^{-2} in April to 2.66 g m^{-2} in August. The linear relationships between N_a and V_{cmax}, J_{max}, TPU and R_d all showed high regression coefficients (r^2 between 0.76 and 0.95).

There were no differences in photosynthetic capacity between I and D plants in April (Figure 4). However, V_{cmax}, J_{max}

Table 2. Values for the olive tree parameters describing the temperature dependence of the maximum catalytic activity of Rubisco in the presence of saturating amounts of RuBP and CO_2 (V_{cmax}); maximum rate of electron transport at saturating irradiance (J_{max}); rate of P_i release associated with triose phosphate utilization (TPU); and rate of CO_2 evolution in the light (R_d) estimated in this work.

Parameter	Value	Units
ΔH_a (V_{cmax})	73.68	kJ mol^{-1}
c (V_{cmax})	33.99	–
ΔH_a (J_{max})	35.35	kJ mol^{-1}
c (J_{max})	18.88	–
ΔH_a (TPU)	30.31	kJ mol^{-1}
c (TPU)	14.02	–
ΔH_a (R_d)	44.79	kJ mol^{-1}
c (R_d)	17.91	–

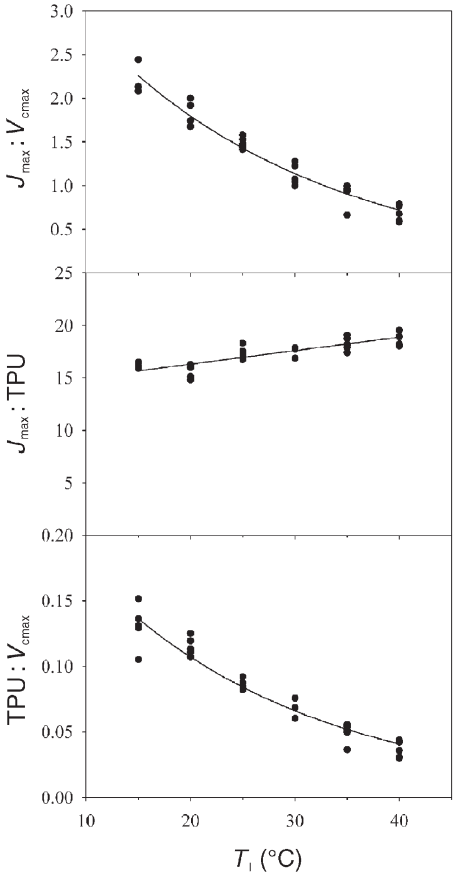

Figure 3. Relationships between photosynthesis model parameters and leaf temperature (T_l): J_{max}:V_{cmax} = 4.48 $e^{-0.0457T_l}$, R^2 = 0.94; J_{max}:TPU = 0.128 T_l + 13.75, r^2 = 0.73; TPU:V_{cmax} = 0.281 $e^{-0.0482T_l}$, R^2 = 0.93. Abbreviations: J_{max} = maximum rate of electron transport at saturating irradiance; V_{cmax} = maximum catalytic activity of Rubisco in the presence of saturating amounts of RuBP and CO_2; and TPU = rate of P_i release associated with triose phosphate utilization.

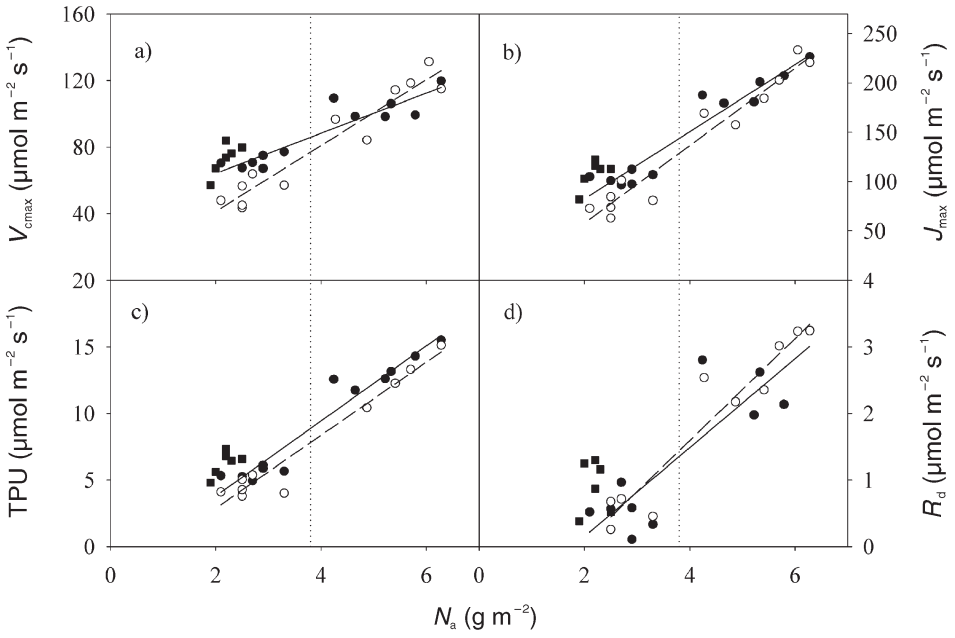

Figure 4. Relationships between photosynthesis model parameters and leaf nitrogen content on an area basis (N_a). Symbols: ■ = measurements on potted plants; ● = field measurements on irrigated trees (I); and ○ = field measurements on non-irrigated trees (D). The dotted line separates measurements made on leaves in spring (on the right) from measurements made on leaves in summer (on the left). (a) I treatment: $V_{cmax} = 12.08N_a + 40.0$, $r^2 = 0.88$; D treatment: $V_{cmax} = 19.77N_a + 1.75$, $r^2 = 0.92$; (b) I treatment: $J_{max} = 34.03N_a + 14.33$, $r^2 = 0.92$; D treatment: $J_{max} = 39.27N_a - 20.66$, $r^2 = 0.94$; (c) I treatment: $TPU = 2.82N_a - 1.84$, $r^2 = 0.93$; D treatment: $TPU = 2.74N_a - 2.62$, $r^2 = 0.95$; (d) I treatment: $R_d = 0.66N_a - 1.18$, $r^2 = 0.76$; and D treatment: $R_d = 0.76N_a - 1.47$, $r^2 = 0.91$. Abbreviations: V_{cmax} = maximum catalytic activity of Rubisco in the presence of saturating amounts of RuBP and CO_2; J_{max} = maximum rate of electron transport at saturating irradiance; TPU = rate of P_i release associated with triose phosphate utilization; and R_d = rate of CO_2 evolution in the light.

and TPU were significantly lower in D plants in August ($P < 0.001$ for V_{cmax} and J_{max}, and $P < 0.005$ for TPU). This resulted in a steeper slope in the linear regression between N_a and V_{cmax} for D plants and, to a lesser extent, with J_{max}. Photosynthetic capacity of the 2-year-old potted plants during August (Figure 4, squares) was similar to that of I trees at the same time of year. There were no significant differences in R_d between I and D plants in April or in August, but R_d was significantly lower in August than in April ($P < 0.001$).

The decrease in N_a was driven by a decrease in leaf mass per unit area (LMA), because N_m varied only slightly (Figure 5). Most of the variance in V_{cmax} was explained by variation in LMA (Figure 5a; Table 3). Values of J_{max}, TPU and R_d were also highly correlated with LMA. Values of N_m did not change significantly between April and August or between treatments, and there was no relationship between V_{cmax} on a leaf mass basis ($V_{cmax,\ m}$) and N_m for the field-grown trees or the 2-year-old plants (Figure 5b). There was a slight decrease in the ratio J_{max}:V_{cmax} in August (1.48) relative to April (1.81) ($P < 0.001$) and J_{max}:V_{cmax} was weakly correlated with LMA. However, there was no difference in J_{max}:V_{cmax} between treatments in April or August.

Seasonal pattern of photosynthesis

Diurnal measurements of photosynthesis showed the typical pattern of species growing in a Mediterranean climate with a maximum rate in the morning followed by a gradual decline over the remainder of the day. On days where VPD was low, a clear midday decrease was less evident. Soil water content increased rapidly when irrigation began at the end of March, resulting in greater differences between treatments during summer (Table 4). At the end of the study, we found significant treatment differences ($P < 0.001$) in variables related to water stress (Ψ_{pd}, Ψ_{min}, RWC and maximum g_s). The differences were not apparent in May, likely because of the 48.0 mm of rainfall that occurred by the middle of the month. Based on the Ψ_w and g_{smax} values, even during the summer months the plants generally experienced only a mild water stress.

Figure 6 shows the comparison between measured and modeled A for both I and D trees from April to August. There was good agreement during most of the study as indicated by the r^2 values and residual mean squared errors (RMSE) (Table 5). When SWC decreased during the dry period, the model correctly predicted the observed reduction in A. The effect of drought was considered in the model by invoking both stomatal and non-stomatal limitations. The effect of soil water stress on A was taken into account by the stomatal conductance sub-model, through effects on the maximum value of g_s. The seasonal decrease in photosynthetic capacity was modeled assuming a linear decay in N_a from April to August, as observed in Figure 4a. This was better simulated by the model for the I trees than for the D trees, as indicated by the value of slope b (i.e., closer to 1; Table 5). For the D trees, high values of A were slightly underestimated by the model; however, RMSE values indicated a more precise model performance for the D trees than for the I plants.

Consequences of coordinated stomatal and photosynthetic capacity adjustments

Table 6 shows a series of closely related variables that provide information about the consequences of adjustment in photosynthetic capacity of olive, as simulated by the model based on

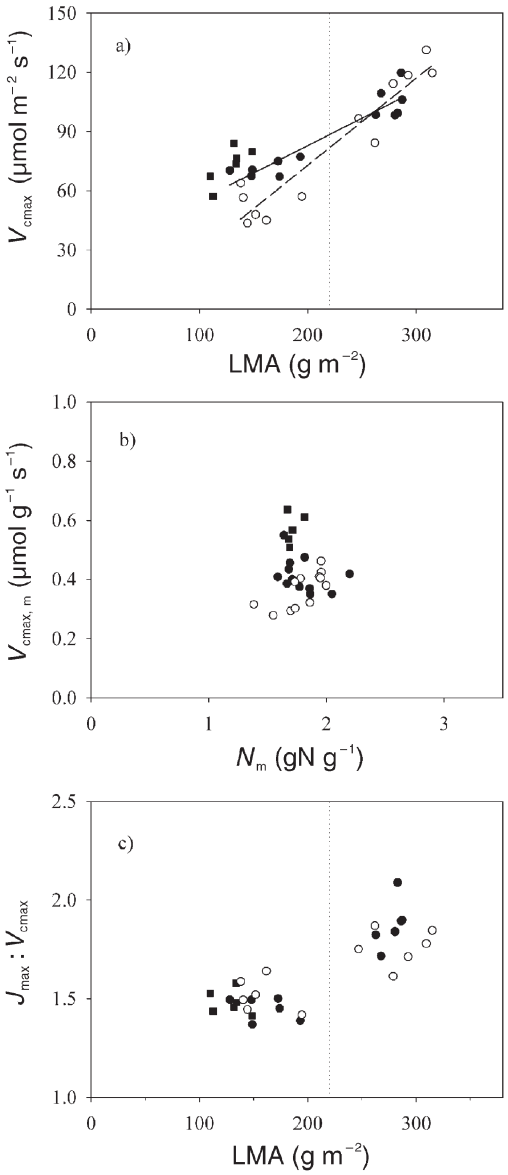

Figure 5. (a) Relationship between photosynthetic capacity of the leaves (V_{cmax}) and their specific mass area (LMA). Dotted line and symbols are as described in Figure 4. (b) Relationship between photosynthetic capacity of the leaves on a mass basis ($V_{cmax, m}$) and their leaf nitrogen content on a mass basis (N_m). (c) Relationship between J_{max}:V_{cmax} ratio and their LMA; J_{max} = maximum rate of electron transport at saturating irradiance.

actual values of N_a measured in I and D trees. Larger l_g in D trees resulted in a larger WUE in D trees compared with I trees. On the other hand, I trees showed a higher NUE than D trees at the expense of decreased WUE, especially in August. Reductions in photosynthetic capacity in August reduced l_g and increased NUE in both treatments, at the expense of reduced WUE. Leaves also performed closer to the transition point between A_c and A_q, where theoretically photosynthetic apparatus resources are optimized. The C_i/C_a ratio was maintained in a narrow range during the season, despite the large decrease in g_s (Figure 7). There was good agreement between the diurnal measured and modeled C_i values. The C_i/C_a ratio was underestimated by 15% when the observed decline in leaf photosynthetic capacity was not included in the calculations (dotted line).

Discussion

There are few published values of V_{cmax} and J_{max} for olive leaves. Bongi and Palliotti (1994) reported a value between 75 and 90 μmol m^{-2} s^{-1} for V_{cmax} at 28 °C, and Centritto et al. (2003) using in vivo parameters obtained a value of V_{cmax} close to the values we found at the same temperature. Bongi and Loreto (1989) analyzed the effects of salt stress and reported a value of J for control plants of 99 μmol m^{-2} s^{-1} at 28 °C and 900 μmol m^{-2} s^{-1} PPF, which is similar to the value we obtained for that irradiance and temperature. Centritto et al. (2003) obtained comparable values for J_{max} once they had removed the effect of diffusional limitation on control and stressed plants. Values for TPU are less frequent in the literature than values for V_{cmax} and J_{max}, and we have found no reference for olive. Wullschleger (1993) reported TPU values for 23 A/C_i response curves of different species. His estimates ranged between 4.9 μmol m^{-2} s^{-1} for the tropical evergreen *Tabebuia rosea* (Bertol.) DC. and 20.1 μmol m^{-2} s^{-1} for the annual weed *Xanthium strumarium* L. The mean for all the species analyzed was 10.1 μmol m^{-2} s^{-1}, which is similar to our mean value at 25 °C.

Observations of TPU limitation have generally been confined to low temperature and to elevated CO_2 concentration (Sage et al. 1989, Lewis et al. 1994, Leegood and Edwards 1996). Our data, however, show that, at high C_i, photosynthesis in olive leaves is insensitive to, or even slightly inhibited by, elevated CO_2 concentration across a range of leaf temperatures

Table 3. Linear regression coefficients for maximum catalytic activity of Rubisco in the presence of saturating amounts of RuBP and CO_2 (V_{cmax}); maximum rate of electron transport at saturating irradiance (J_{max}); rate of P_i release associated with triose phosphate utilization (TPU); and rate of CO_2 evolution in the light (R_d) versus leaf mass per unit area.

	Irrigated trees			Non-irrigated trees		
	Intercept	Slope	r^2	Intercept	Slope	r^2
V_{cmax}	27.33	0.277	0.88	– 15.27	0.44	0.90
J_{max}	– 17.08	0.763	0.91	– 52.56	0.863	0.92
TPU	– 4.5	0.063	0.93	– 4.38	0.059	0.86
R_d	– 1.88	0.015	0.78	– 1.87	0.016	0.90

Table 4. Environmental and physiological variables measured in the field for the irrigation (I) and non-irrigation (D) trees for the days reported in Figure 6. Abbreviations: SWC = volumetric soil water content ($m^3\ m^{-3}$); VPD_{max} = maximum water vapor pressure deficit of the air (kPa); P = precipitation (mm); RWC_{min} = minimum relative water content of the leaves (%); Ψ_{pd} = predawn leaf water potential (MPa); Ψ_{min} = minimum leaf water potential measured (MPa); and g_{smax} = maximum stomatal conductance measured in the day (mol $m^{-2}\ s^{-1}$). For each variable, values with different letters are significantly different ($P < 0.05$, $n = 6$–10).

Variable	Treatment	March	April	May	June	July	August
SWC	I	0.15 a	0.19 a	0.18 a	0.19 a	0.18 a	0.19 a
	D	0.16 a	0.16 b	0.17 a	0.16 b	0.14 b	0.14 b
VPD_{max}		2.81	2.65	1.8	2.57	2.64	3.01
P		21.5	22.5	48.0	16.0	0.0	0.0
RWC_{min}	I	–	84.70 a	88.76 a	85.13 a	84.12 a	84.57 a
	D	–	83.94 a	87.60 a	85.0 a	84.78 a	80.64 b
Ψ_{pd}	I	–0.17 a	–0.34 a	–0.25 a	–0.13 a	–0.24 a	–0.35 a
	D	–0.19 a	–0.34 a	–0.21 a	–0.16 a	–0.37 b	–0.57 b
Ψ_{min}	I	–1.60 a	–1.75 a	–1.77 a	–1.92 a	–2.39 a	–2.63 a
	D	–1.52 a	–1.90 b	–1.79 a	–2.22 b	–2.38 a	–2.87 b
g_{smax}	I	0.148 a	0.206 a	0.218 a	0.207 a	0.206 a	0.226 a
	D	0.143 a	0.169 b	0.206 a	0.202 a	0.183 b	0.174 b

from 15 to 35 °C or 40 °C. Data on TPU-limited photosynthesis across such a broad temperature range are rare, and our data allowed the temperature dependence of TPU to be quantified. At ambient CO_2 concentration, we observed TPU-limited photosynthesis at 15 °C when stomata were fully open. In some leaves, there was a direct transition from a limitation by A_c to a limitation by A_p. These data suggest that olive invests fewer resources in TPU relative to electron transport capacity than most other species. We found published evidence of TPU limitation only at higher temperatures in grapevines (Schultz 2003). In our case, the limitation may be related to a decrease in the export of sucrose, perhaps associated with reduced N metabolism, or simply reduced growth rate during drought.

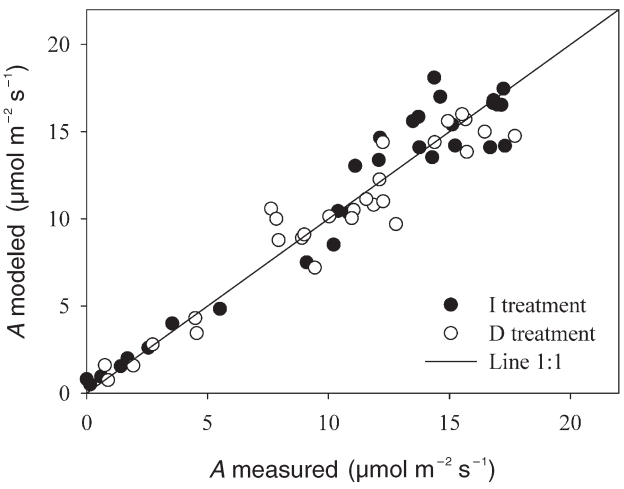

Figure 6. Comparison between modeled and measured photosynthetic rate (A) in irrigated trees (I; ●) and non-irrigated trees (D; ○) from March to August. Each value is the mean of 10 measurements. The model was run with environmental data from the meteorological station.

Sucrose and starch syntheses are tightly coupled to the rate of CO_2 assimilation via the exchange of triose phosphate and inorganic phosphate across the chloroplast envelope membrane (Foyer et al. 2000). Maroco et al. (2002) related the reduction in utilization of triose phosphate in grapevines in response to drought with the slowdown in growth observed in water-stressed plants.

The values of the parameters that explain the temperature response of Rubisco activity and RuBP-limited photosynthesis in olive (Table 2) did not differ significantly from those published by Bernacchi et al. (2001, 2003), and fall within the range of values for evergreen trees reported by Medlyn et al. (2002*a*). This indicates the robustness of these parameters calculated in vivo and applied to a range of species. We did not find a clear optimum temperature for V_{cmax}, J_{max} or TPU, probably because the maximum temperature we measured was 40 °C, and olive is adapted to this and even higher temperatures during summer. Dreyer et al. (2001) analyzed the temperature response of seven temperate tree species and found that the optimum temperature was above 40 °C for many of the species. They also concluded that J_{max} had a lower optimum temperature than V_{cmax}. This agrees with our finding in olive based on a deactivation energy parameter.

Relationships between V_{cmax}, J_{max} and TPU are important for

Table 5. Results of the linear regression ($y = a + bx$) of observed and estimated leaf photosynthesis for the model in olive leaves from April to August. At least six values per month were used in the regression. Each value is the mean of 10 measurements.

Treatment	a	b	r^2	RMSE
I	0.512	0.97	0.94	2.23
D	0.88	0.89	0.94	1.72
Both	0.94	0.94	0.97	2.01

Table 6. Model outputs for water-use efficiency (WUE, μmol CO_2 mmol H_2O^{-1}), nitrogen-use efficiency (NUE, μmol CO_2 mol N^{-1} s^{-1}), percentage of stomatal limitation (l_g, %), and transition point between photosynthesis limited by carboxylation rate and electron transport rate, expressed as the ratio between A_c and A_q. All the values represent the daily means excluding early morning and late evening when photosynthetically active radiation was < 500 μmol m^{-2} s^{-1} for both water treatments: irrigated (I) and dry-farming (D).

Month	WUE		NUE		l_g		A_c:A_q	
	I	D	I	D	I	D	I	D
April	4.92	5.6	46.30	40.45	38.5	44.5	1.15	1.12
August	4.2	5.19	76.22	49.54	32.4	39.4	1	1.09

the coupling of processes related to light harvesting and carboxylation capacity (Wullschleger 1993). Such relationships have been used by some modelers to estimate J_{max} from V_{cmax} measurements (Williams et al. 1996). The J_{max}:TPU ratio changed little with temperature, indicating that these parameters are affected by temperature in a similar way. The J_{max}:V_{cmax} ratio decreased slightly, but significantly, from April to August (Figure 5c). Medlyn et al. (2002*b*) found a decrease in J_{max}:V_{cmax} in maritime pine in a summer survey, although they could not explain it by ambient temperature, N content or needle age. One possible explanation is that there is relatively less investment in electron transport later in the season when drought is severe than at earlier stages. The amount of solar energy potentially absorbed by leaves is higher in summer than in spring, but the greater stomatal limitation often imposed during summer means that photosynthesis is more likely to be limited by RuBP carboxylation than RuBP regeneration, therefore requiring less investment in RuBP regeneration. In summer at high temperatures, leaves with a reduced transpirational cooling capacity need to acclimate the electron transport apparatus (Medlyn et al. 2002*b*), and probably, as with many species under Mediterranean summer conditions, enhance other mechanisms of light energy dissipation (Flexas and Medrano 2002*a*).

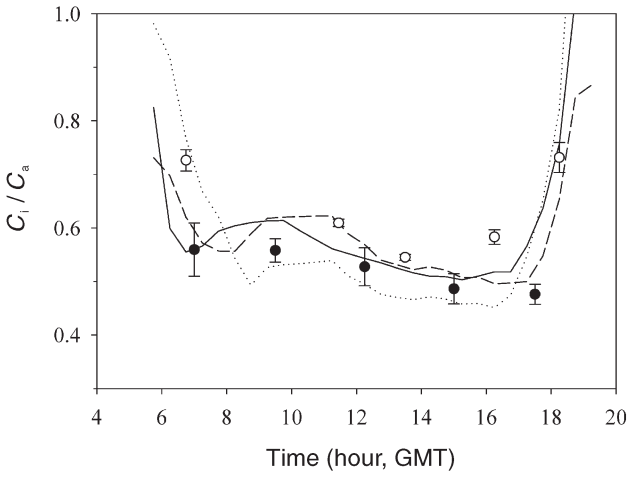

Figure 7. Ratio of C_i/C_a (where C_i is the intercellular CO_2 mole fraction and C_a is the mole fraction of CO_2 in ambient air) for the D treatment in April (●) and August (○), and the modeled C_i/C_a (April, solid line; August, broken line; August with no photosynthetic capacity adjustment, dotted line). Each value is the mean of 10 measurements. Vertical bars represent one standard error. Abbreviation: GMT = Greenwich Mean Time.

We found a clear seasonal reduction in the photosynthetic capacity of olive leaves (Figure 4). Our data show that the primary cause of the decline in photosynthetic capacity was not drought. Leaves in both treatments showed a decreased photosynthetic capacity, although the decline was slightly greater for D trees than for I trees. The small difference represents the drought effect. When the observed reduction in photosynthetic capacity due to drought (based on the decrease in N_a) was included in the model, we obtained a satisfactory fit of the simulated data to the field data throughout the season. The reduction in photosynthetic capacity was strongly related to the reduction in N_a, showing a 2-fold decrease for a similar decrease in N_a. The reduction in N_a was also correlated to a decrease in LMA. When photosynthetic capacity was expressed on a leaf mass basis, there was no significant difference between leaves in April and August. A similar result was reported by Sims and Pearcy (1992). Many authors have reported a reduction in photosynthetic capacity related to LMA (Wilson et al. 2000, Le Roux et al. 2001, Walcroft et al. 2002). However, in all these studies the reduction in LMA was interpreted as an acclimation response to reduced irradiance of shaded foliage. Our measurements were made in the outer part of the canopy, and therefore leaf irradiance in summer was higher than in spring. It is unlikely, therefore, that the observed reduction in LMA can be attributed to light acclimation. Wirtz (2000) modeled seasonal changes in LMA in beech using an approach based on the optimization of growth rate, which is largely dependent on A. Wirtz (2000) predicted that a reduction in A due to stomatal limitation could affect the growth rate of the new foliage, thereby reducing LMA. We observed a decrease in maximum g_s throughout the growing season (Table 4) that was responsible for up to 50% of the limitation of photosynthesis observed in summer.

The C_i/C_a ratio was maintained within a narrow range throughout the season (Figure 7) and reflects tight coupling between A and g_s. A close relationship between these variables has also been shown by Flexas et al. (2001) for *Pistacia lentiscus*, another Mediterranean woody plant, who concluded that both stomatal and non-stomatal limitations play a role in the response to drought. Our data indicate that both stomatal and non-stomatal limitations must be considered when modeling photosynthesis in olive. Our model also shows that the C_i

at which olive leaves operated coincided with the transition point between photosynthetic limitation due to RuBP carboxylation and that due to RuBP regeneration. Some authors have suggested that at this point allocation of N between the light-harvesting apparatus and carboxylation capacity is most efficient (von Caemmerer and Farquhar 1981). Decreases in both stomatal conductance and photosynthetic capacity during summer imply that olive plants maintain a relatively constant value of C_i, and operate around the transition point.

Our results provide support for the suggested trade-off between NUE and WUE (Field et al. 1983, Chen et al. 2005). In summer, well-watered plants showed a marked increase in NUE, at the expense of a reduction in WUE (Table 6). A similar but reduced trend was observed in D trees. In both I and D trees, N_a declined during summer, which greatly reduced the photosynthetic capacity of leaves (see Figure 4). However, to evaluate the effect of this reduction on A we must consider the operating range of g_s in each treatment, and in this context the highest value of NUE shown by I trees was associated with a greater g_s during summer. Evergreen woody plants in the Mediterranean basin typically show a highly conservative resource-use strategy, and it has been considered an adaptation to low-nutrient availability (Valladares et al. 2000). This could explain why even in D trees, which were subjected to moderate water stress, leaves still preferentially optimized NUE instead of WUE.

It is necessary, however, to consider some uncertainties when estimating photosynthetic capacity of leaves from A/C_i response curves. The observed decrease in photosynthetic capacity estimated from the analysis of A/C_i response curves may be confounded by three main problems: changes in cuticular conductance to vapor pressure; patchy stomatal closure; and increased mesophyll resistance (Flexas and Medrano 2002*b*). The conductance of the waxy cuticle of olive leaves is negligible, and it is assumed that the total conductance to water vapor is essentially equal to g_s plus boundary layer conductance. An effect of stomatal patchiness was unlikely because steps were taken to avoid the sources of patchiness in olive detected by Loreto and Sharkey (1990). Centritto et al. (2003) and Loreto et al. (2003) showed that the observed reduction in photosynthetic capacity in leaves of salt-stressed olive was artificial and a consequence of a reduction in mesophyll conductance (g_m). They also observed that changes in g_m can be as rapid as changes in g_s.

Some of these factors may have affected our measurements; however, the observed proportional decrease in N_a indicates that the reduction in the measured photosynthetic capacity was real and not an artefact. Furthermore, field trees were generally subjected to a progressive increase in drought conditions, and the development of new foliage adjusted to the seasonal changes of the environment. Reductions in V_{cmax} during drought were reported for a deciduous forest (Wilson et al. 2000), suggesting that drought-induced growth limitation can result in sink limitation and feedback control on photosynthetic capacity. Medlyn et al. (2002*b*) also showed a seasonal decrease in V_{cmax} and J_{max} in *Pinus pinaster* Ait. that was related to temperature acclimation. Maroco et al. (2002) found that, in grapevines under slowly imposed drought stress, although stomatal closure was a strong limitation to CO_2 assimilation, comparable reductions in electron transport, CO_2 carboxylation and utilization of triose-P capacities also occurred.

By combining the leaf-level model outlined in this paper with a model of radiation transfer through the canopy, we aim to scale-up predictions of photosynthesis and transpiration to the tree crown level. Preliminary data for whole olive tree photosynthesis has already been published (Diaz-Espejo et al. 2002), but more information about the spatial and temporal distributions of radiation and photosynthetic capacity of olive leaves is needed. The incorporation of the effect of soil water content on stomatal control of transpiration, and its consequences for limiting photosynthesis, makes the model a potential tool for predicting the response of whole-tree carbon assimilation to water stress, and thereby determining management strategies to optimize production and the use of irrigation water.

Acknowledgments

We thank the staff of La Hampa for managing the orchard. Financial support was provided by Spanish CICYT, Project HID96-342-CO4-01, and an MEC fellowship to Antonio Diaz-Espejo. We thank Dr. Jose María Romero from the Instituto de Bioquímica Vegetal y Fotosíntesis for the use of the Fitotron chamber, and to Dr. José Enrique Frías for technical support. We also thank Dr. T.D. Sharkey for valuable comments on TPU limitation of photosynthesis on an earlier version of this manuscript.

References

Angelopoulos, K., B. Dichio and C. Xiloyannis. 1996. Inhibition of photosynthesis in olive trees (*Olea europaea* L.) during water stress and rewatering. J. Exp. Bot. 47:1093–1100.

Badger, M.R. and G.J. Collatz. 1977. Studies on the kinetic mechanism of ribulose 1-5-biphosphate carboxylase and oxygenase reactions, with particular reference to the effect of temperature on kinetic parameters. Carnegie Inst. Washington Year Book 76: 355–361.

Bernacchi, C.J., E.L. Singsaas, C. Pimentel, A.R. Portis and S.P. Long. 2001. Improved temperature response functions for models of RuBisCO-limited photosynthesis. Plant Cell Environ. 24: 253–259.

Bernacchi, C.J., C. Pimentel and S.P. Long. 2003. In vivo temperature response functions of parameters required to model RuBP-limited photosynthesis. Plant Cell Environ. 26:1419–1430.

Bongi, G., M. Mencuccini and G. Fontanazza. 1987. Photosynthesis of olive leaves: effect of light flux density, leaf age, temperature, peltates, and H_2O vapor pressure deficit on gas exchange. J. Am. Soc. Hortic. Sci. 112:143–148.

Bongi, G. and F. Loreto. 1989. Gas-exchange properties of salt-stressed olive (*Olea europaea* L.) leaves. Plant Physiol. 90: 1408–1416.

Bongi, G. and A. Palliotti. 1994. Olive. *In* Handbook of Environmental Physiology of Fruit Crops. Vol. I: Temperate Crops. Eds. B. Schaffer and P.C. Andersen. CRC Press, Boca Raton, FL, pp 165–187.

Centritto, M., F. Loreto and K. Chartzoulakis. 2003. The use of low [CO_2] to estimate diffusional and non-diffusional limitations of photosynthetic capacity of salt-stressed olive saplings. Plant Cell Environ. 26:585–594.

Chen, S., Y. Bai, L. Zhang and X. Han. 2005. Comparing physiological responses of two dominant grass species to nitrogen addition in Xilin River Basin of China. Environ. Exp. Bot. 53:65–75.

Dichio, B., V. Nuzzo, C. Xiloyannis and K. Angelopoulos. 1997. Drought stress-induced variation of pressure–volume relationships in *Olea europaea* L. cv 'Coratina'. Acta Hort. 442:401–409.

Díaz-Espejo, A., B. Hafidi, J.E. Fernández, M.J. Palomo and H. Sinoquet. 2002. Transpiration and photosynthesis of the olive tree: a model approach. Acta Hort. 586:457–460.

Dreyer, E., X. Le Roux, P. Montpied, F.A. Daudet and F. Masson. 2001. Temperature response of leaf photosynthetic capacity in seedlings from seven temperate tree species. Tree Physiol. 21: 223–232.

Farquhar, G.D., S. von Caemmerer and J.A. Berry. 1980. A biochemical model of photosynthetic CO_2 assimilation in leaves of C_3 species. Planta 149:78–90.

Farquhar, G.D. and S.C. Wong. 1984. An empirical model of stomatal conductance. Aust. J. Plant Physiol. 11:191–210.

Fergusson, L. 2000. Current physiological and biological research on olives. 4th Int. Symp. on Olive Growing. ISHS. Valenzano, Italy, 79 p.

Fernández, J.E. and F. Moreno. 1999. Water use by the olive tree. J. Crop Prod. 2:101–162.

Fernández, J.E., F. Moreno, I.F. Girón and O.M. Blázquez. 1997. Stomatal control of water use in olive tree leaves. Plant Soil 190: 179–192.

Field, C., J. Merino and H.A. Mooney. 1983. Compromises between water-use efficiency and nitrogen-use efficiency in five species of California evergreens. Oecologia 60:384–389.

Flexas, J., J. Gulías, S. Jonasson, H. Medrano and M. Mus. 2001. Seasonal patterns and control of gas exchange in local populations of the Mediterranean evergreen shrub *Pistacia lentiscus* L. Plant Cell Environ. 22:33–43.

Flexas, J. and H. Medrano. 2002*a*. Energy dissipation in C_3 plants under drought. Funct. Plant Biol. 29:1209–1215.

Flexas, J. and H. Medrano. 2002*b*. Photosynthetic responses of C_3 plants to drought. *In* Advances in Plant Physiology. Vol. 4. Ed. A. Hemantaranjan. Scientific Publishers, Jodhpur, India, pp 1–56.

Foyer, C.H., S. Ferrario-Méry and S.C. Huber. 2000. Regulation of carbon fluxes in the cytosol: coordination of sucrose synthesis, nitrate reduction and organic acid and amino acid biosynthesis. *In* Photosynthesis: Physiology and Metabolism. Eds. R.C. Leegood, T.D. Sharkey and S. von Caemmerer. Kluwer Academic Publishers, The Netherlands, pp 177–203.

Gary, C., J.W. Jones and M. Tchamitchian. 1998. Crop modeling in horticulture: state of the art. Sci. Hortic. 74:3–20.

Goldhamer, D.A., J. Dunai and L.F. Ferguson. 1994. Irrigation requirements of olive trees and responses to sustained deficit irrigation. Acta Hort. 356:172–175.

Harley, P.C. and J.D. Tenhunen. 1991. Modeling the photosynthetic response of C_3 leaves to environmental factors. *In* Symposium on Modeling Crop Photosynthesis—From Biochemistry to Canopy. Eds. K.J. Boote and R.S. Loomis. CSSA Special Publication No. 19, American Society of Agronomy and Crop Science Society of America, Madison, WI, pp 17–39.

Jarvis, P.G. 1976. The interpretation of the variation in leaf water potential and stomatal conductance found in canopies in the field. Philos. Trans. Roy. Soc. Lond. Biol. Sci. 273:593–610.

Jones, H.G. 1992. Plants and microclimate. Cambridge Univ. Press, New York, 323 p.

Larsen, F.E., S.S. Higgins and A. Al Wir. 1989. Diurnal water relations of apple, apricot, grape, olive and peach in an arid environment (Jordan). Sci. Hort. 39:211–222.

Lavee, S., M. Nashef, M. Wodner and H. Harshemesh. 1990. The effect of complementary irrigation added to old olive trees (*Olea europaea* L.) cv. 'Souri' on fruit characteristics, yield and oil production. Adv. Hort. Sci. 4:135–138.

Leegood, R.C. and G.E. Edwards. 1996. Carbon metabolism and photorespiration: temperature dependence in relation to other environmental factors. *In* Photosynthesis and the Environment. Ed. N.R. Baker. Kluwer Academic Publishers, Dordrecht, pp 191–221.

Le Roux, X., A.S. Walcroft, F.A. Daudet, H. Sinoquet, M.M. Chaves, A. Rodrigues and L. Osorio. 2001. Photosynthetic light acclimation in peach leaves: importance of changes in mass:area ratio, nitrogen concentration, and leaf nitrogen partitioning. Tree Physiol. 21:377–386.

Leuning, R. 1995. A critical appraisal of a combined stomatal–photosynthesis model for C_3 plants. Plant Cell Environ. 18:339–355.

Lewis, J.D., K.L. Griffin, R.B. Thomas and B.R. Strain. 1994. Phosphorus supply affects the photosynthetic capacity of loblolly pine grown in elevated carbon dioxide. Tree Physiol. 14:1229–1244.

Loreto, F. and T.D. Sharkey. 1990. Low humidity can cause uneven photosynthesis in olive (*Olea europaea* L.) leaves. Tree Physiol. 6:409–415.

Loreto, F., M. Centritto and K. Chartzoulakis. 2003. Photosynthesis limitations in olive cultivars with different sensitivity to salt stress. Plant Cell Environ. 26:595–601.

Mariscal, M.J., F. Orgaz and F. Villalobos. 2000*a*. Modeling and measurement of radiation interception by olive canopies. Agric. For. Meteorol. 100:183–197.

Mariscal, M.J., F. Orgaz and F. Villalobos. 2000*b*. Radiation-use-efficiency and dry matter partitioning of a young olive (*Olea europaea*) orchard. Tree Physiol. 20:65–72.

Maroco, J.P., M.L. Rodrigues, C. Lopes and M.M. Chaves. 2002. Limitations to leaf photosynthesis in field-grown grapevine under drought—metabolic and modeling approaches. Funct. Plant Biol. 29:451–459.

Medlyn, B.E., E. Dreyer, D.S. Ellsworth et al. 2002*a*. Temperature responses of parameters of a biochemically-based model of photosynthesis. II. A review of experimental data. Plant Cell Environ. 25:1167–1179.

Medlyn, B.E., D. Loustau and S. Delzon. 2002*b*. Temperature response of parameters of a biochemically based model of photosynthesis. I. Seasonal changes in mature maritime pine (*Pinus pinaster* Ait.). Plant Cell Environ. 25:1155–1165.

Michelakis, N., E. Vouyoukalou and G. Clapaki. 1996. Water use and soil moisture depletion by olive trees under different irrigation conditions. Agric. For. Meteorol. 29:315–325.

Moreno, F., J.E. Fernández, B.E. Clothier and S.R. Green. 1996. Transpiration and root water uptake by olive trees. Plant Soil 184:85–96.

Moriana, A., F.J. Villalobos and E. Fereres. 2002. Stomatal and photosynthetic responses of olive (*Olea europaea* L.) leaves to water deficits. Plant Cell Environ. 25:395–405.

Palomo, M.J., F. Moreno, J.E. Fernández, A. Diaz-Espejo and I.F. Girón. 2002. Determining water consumption in olive orchards using the water balance approach. Agric. Water Manage. 55:15–35.

Pokovai, K. and G.J. Kovacs. 2003. Development of crop models: a critical review. Novenytermeles 52:573–582.

Sage, R.F., T.D. Sharkey and J.R. Seeman. 1989. Acclimation of photosynthesis to elevated CO_2 in five C_3 species. Plant Physiol. 84: 590–596.

Schultz, H.R. 2003. Extension of a Farquhar model for limitations of leaf photosynthesis induced by light environment, phenology and leaf age in grapevines (*Vitis vinifera* L. cv. 'White Riesling' and 'Zinfandel'). Funct. Plant Biol. 30:673–687.

Sims, D.A. and R.W. Pearcy. 1992. Response of leaf anatomy and photosynthetic capacity in *Alocasia macorrhiza* (Araceae) to a transfer form low to high light. Am. J. Bot. 79:449–455.

Tombesi, A., P. Proietti and G. Nottiani. 1984. Effect of water stress on photosynthesis, transpiration, stomatal resistance and carbohydrate level in olive trees. Olea 17:35–40.

Valladares, F., E. Martinez-Ferri, L. Balaguer, E. Perz-Corona and E. Manrique. 2000. Low leaf-level response to light and nutrients in Mediterranean evergreen oaks: a conservative resource-use strategy? New Phytol. 148:79–91.

Villalobos, F.J., F. Orgaz, L. Testi and E. Fereres. 2000. Measurement and modeling of evapotranspiration of olive (*Olea europaea* L.) orchards. Eur. J. Agric. 13:155–163.

von Caemmerer, S. and G.D. Farquhar. 1981. Some relationships between the biochemistry of photosynthesis and the gas exchange of leaves. Planta 153:376–387.

Walcroft, A.S., X. Le Roux, A. Diaz-Espejo, N. Dones and H. Sinoquet. 2002. Effects of crown development on leaf irradiance, leaf morphology and photosynthetic capacity in a peach tree. Tree Physiol. 22:929–938.

Wang, Y.P. and P.G. Jarvis. 1993. Influence of shoot structure on the photosynthesis of Sitka spruce (*Picea sitchensis*). Funct. Ecol. 7: 433–451.

Williams, M., E.B. Rastetter, D.N. Fernades, M.L. Goulden, S.C. Wofsy, G.R. Shaver, J.M. Melillo, J.W. Munger, S.-M. Fan and K.J. Nadelhoffer. 1996. Modeling the soil-plant-atmosphere continuum in a *Quercus–Acer* stand at Harvard forest: the regulation of stomatal conductance by light, nitrogen and soil/plant hydraulic properties. Plant Cell Environ. 19:911–927.

Wilson, K.B., D.D. Baldocchi and P.J. Hanson. 2000. Spatial and seasonal variability of photosynthetic parameters and their relationship to leaf nitrogen in a deciduous forest. Tree Physiol. 20: 565–578.

Wirtz, K.W. 2000. Simulating the dynamics of leaf physiology and morphology with an extended optimality approach. Ann. Bot 86: 753–764.

Wullschleger, S.D. 1993. Biochemical limitations to carbon assimilation in C_3 plants—a retrospective analysis of the A/C_i curves from 109 species. J. Exp. Bot. 44:907–920.

Appendix

Stomatal conductance g_s is computed following the empirical model of Jarvis (1976) as:

$$g_s = g_{sref}\, f(Q)\, f(T_l)\, f(\mathrm{VPD})\, f(\theta) \quad \text{(A1)}$$

where each function f describes the relative importance of its control on g_s, and g_{sref} is the reference stomatal conductance observed under standard conditions (PPF = 1600 μmol m^{-2} s^{-1}, T_l = 25 °C; VPD_s = 1 kPa and θ = 0.21 m^3 m^{-3}).

The effect of incident photosynthetically active photon flux (PPF) on stomatal conductance is described as:

$$f(Q) = 0.081 + 0.9(1 - e^{-0.003Q}) \quad \text{(A2)}$$

The effect of leaf temperature (T_l) on stomatal conductance is described as:

$$f(T_l) = -0.11 + 0.07T_l - 9.67 \times 10^{-4} T_l^2 \quad \text{(A3)}$$

The effect of air water vapor pressure deficit at the olive leaf surface (VPD_s) did not show a significant response to VPD_s until VPD_s was higher than 1.5 kPa;

$$f(\mathrm{VPD}_s) = 1.3\,\mathrm{VPD}_s^{-0.8}, \text{ if } \mathrm{VPD}_s > 1.5 \quad \text{(A4)}$$

$$f(\mathrm{VPD}_s) = 1, \text{ if } \mathrm{VPD}_s < 1.5 \quad \text{(A5)}$$

The sigmoidal response of g_s to soil water content (θ) is described as:

$$f(\theta) = 0.38 + \frac{0.8\theta^{13.63}}{0.19^{13.63} + \theta^{13.63}} \quad \text{(A6)}$$

Figure A1 shows a comparison between simulated g_s and measured g_s for the period corresponding to the period over which photosynthesis was simulated.

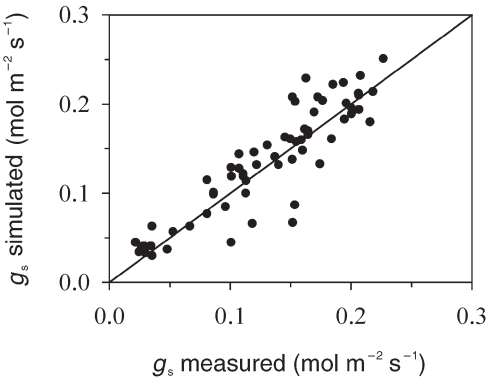

Figure A1. Comparison of simulated g_s with measured g_s for the period corresponding to the simulation of photosynthesis. Months from March to April and leaves from both irrigation treatments are included in the plot.